

CHEM_{NANO}MAT

CHEMISTRY OF NANOMATERIALS FOR ENERGY, BIOLOGY AND MORE

www.chemnanomat.org

Accepted Article

Title: Trimetallic nanoparticles encapsulated into Bamboo-Like N-Doped Carbon Nanotube as a Robust Catalyst for Efficient Oxygen Evolution Electrocatalysis

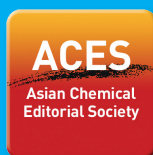
Authors: Mengting Lu, Yuwen Li, Yuhang Wu, Hui Xu, Junkuo Gao, and Shiqing Xu

This manuscript has been accepted after peer review and appears as an Accepted Article online prior to editing, proofing, and formal publication of the final Version of Record (VoR). This work is currently citable by using the Digital Object Identifier (DOI) given below. The VoR will be published online in Early View as soon as possible and may be different to this Accepted Article as a result of editing. Readers should obtain the VoR from the journal website shown below when it is published to ensure accuracy of information. The authors are responsible for the content of this Accepted Article.

To be cited as: *ChemNanoMat* 10.1002/cnma.202000365

Link to VoR: <https://doi.org/10.1002/cnma.202000365>

A Journal of



A sister journal of *Chemistry – An Asian Journal*
and *Asian Journal of Organic Chemistry*

WILEY-VCH

Trimetallic nanoparticles encapsulated into Bamboo-Like N-Doped Carbon Nanotube as a Robust Catalyst for Efficient Oxygen Evolution Electrocatalysis

Mengting Lu^{1,2}, Yuwen Li², Yuhang Wu², Hui Xu^{1*}, Junkuo Gao^{2*}, Shiqing Xu^{1*}

¹Institute of Optoelectronic Materials and Devices, Key Laboratory of Rare Earth Optoelectronic Materials and Devices of Zhejiang Province, China Jiliang University, Hangzhou 310018, China.

²Institute of Fiber based New Energy Materials, The Key Laboratory of Advanced Textile Materials and Manufacturing Technology of Ministry of Education, College of Materials and Textiles, Zhejiang Sci-Tech University, Hangzhou 310018, China

Corresponding Author

H. Xu: huixu@cjlu.edu.cn;

J. Gao: jkgao@zstu.edu.cn;

S. Xu: shiqingxu75@163.com

Keywords: Electrocatalysis; Coordination Polymers; Trimetallic doping; Bamboo-like structure; Oxygen evolution reaction;

Abstract:

High-efficiency oxygen evolution reaction (OER) electrocatalyst based on transition metal materials are one of the most promising alternatives, but their activity and durability are still far from desirable. Here, we report a trimetallic N-doped carbon nanotubes with rapid electron transport and rapid diffusion of the electrolyte that can significantly enhance the OER. The introduction of a third metal can adjust the electronic structure, thereby causing favorable intermediate adsorption on the catalysts. The optimized catalyst CoFeNi@CNTs exhibits a low overpotential of 287 mV at 10 mA cm⁻² and a small Tafel slope of 32 mV dec⁻¹, which are obviously superior to the precious catalyst IrO₂ and most previous reported catalysts. The CoFeNi@CNTs also exhibit excellent OER stability with small current density decay after 12 h. The outstanding OER activity ascribed to the unique carbon nanotube structure and strong synergy between three metals.

Introduction:

It is highly urgent to explore renewable and green energy technologies, such as fuel cells, water splitting systems which hold great prospect towards solving the energy depletion and the aggravation of environment pollution^[1]. And oxygen evolution reaction (OER) is deemed as the core processes in these renewable energy technologies. However, owing to the multistep proton-coupled electron transfer, the kinetics of OER is sluggish, limiting the efficiency of the electrochemical systems^[2]. Currently, Ir/Ru-base compounds show decent activity in OER^[3]. However, their exorbitant price and scarcity extremely impede the large-scale utilization as well as the practical application. To this end, it is extremely urgent to design rationally and synthesize non-precious metal-based electrocatalysts with

outstanding performance for the OER.

During the past years, the first row of transition metals (3d TMs, such as Fe, Co, and Ni) have been used widely in the design and synthesis of efficient non-precious-metal oxygen electrocatalysts on account of their low price and abundant resources^[4-7]. What's more, the obtained catalysts due to the superior performance also play an important role in the field of energy storage^[8-9]. For instance, Wang et. al designed a bifunctional oxygen electrode composed of spinel $\text{Co}_2\text{FeO}_4/(\text{Co}_{0.72}\text{Fe}_{0.28})\text{Td}(\text{Co}_{1.28}\text{Fe}_{0.72})_{\text{Oct}}\text{O}_4$ nanoparticles grown on N-doped carbon nanotubes (NCNTs)^[9]. The catalyst exhibits excellent oxygen electrocatalysis performance and can be used for Zinc-air batteries. However, the individual active centers and insufficient transfer efficiency hinder their practical application. Currently, tailoring the composition of transition metal-based compounds (such as incorporating heteroatoms or foreign metal atoms into the lattice) and constructing high-speed diffusion channels are widely deemed as effective strategies to design electrocatalysts^[10-15]. For example, Yuan et. al suggested a facile supersaturated co-precipitation method to synthesize amorphous NiFeMo oxides with uniform distribution of elements. The obtained catalysts exhibited superior OER activity with an overpotential of 280 mV at 10 mA cm^{-2} ^[16]. In this way, the structural and electronic structure of the host material are regulated elegantly and the interaction between various components can produce additional synergistic effects for better electrochemical performance. At the same time, the high-speed channel allows sufficient charges (electrons and ions) to be transferred to the accessible mobile location in a timely manner. CNTs with large specific surface area and high electrical conductivity can facilitate electron and ion transport, especially the N-doped CNTs. Many pioneers work has demonstrated that the electron-rich N atoms can tailor charge density and spin

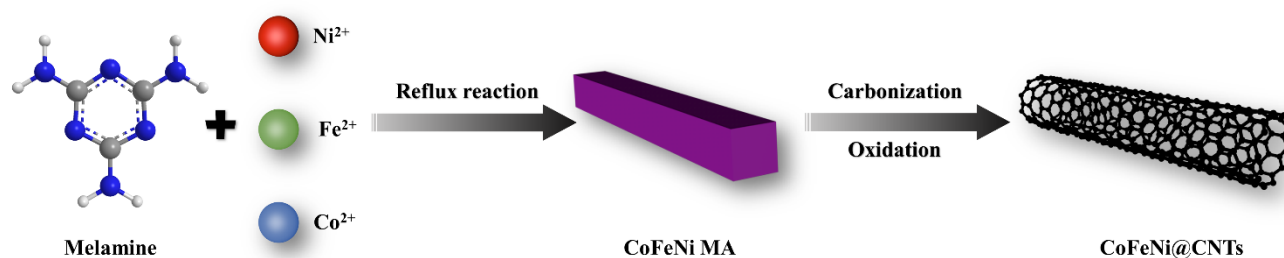
density of carbon atoms in the crystal lattice thus enhance electrical conductivity^[17-20]. Moreover, encapsulating metals or their alloy nanoparticles (NPs) encapsulating in N-doped carbon nanotubes (CNTs) show remarkable performance for electrocatalysis due to the interaction between NPs and CNTs^[21-23]. However, there are few reports of metal compounds having multiple active sites in N-doped carbon nanotubes.

Coordination polymers, or metal-organic frameworks (MOFs) have been approved to be ideal precursors and templates for carbon-based nanocomposites due to their intrinsic well-tunable chemical structures and morphologies, high porosity, as well as large specific surface areas^[24-28]. Moreover, after pyrolysis under the inert gas atmosphere, the heteroatom (such as N, P, S) doped organic ligands in MOFs will be directly converted into heteroatom-doped porous carbon without additional treatment^[29]. For example, Ning et. al used bimetallic MOFs composite as the precursor to prepare the porous N-doped carbon encapsulated CoNi alloy nanoparticle composite (CoNi@N-C)^[30]. Although various N-doped CNTs (NCNTs) structures derived from MOFs have been reported as OER electrocatalysts, the electrochemical activity of most of them still need improvement^[31-33].

In this study, we focused on improving the catalytic performance of the catalyst by adjusting the electronic structure and encapsulating the active nanoparticles in the N-doped carbon nanotube to significantly boost electrochemical performance and stability. Consequently, the obtained catalyst CoFeNi@CNTs delivered a low overpotential of 287 mV to achieve 10 mA cm⁻² and a small Tafel slope of 32 mV dec⁻¹, obviously superior to the commercial IrO₂ and most previous reported catalysts^[34-38]. The CoFeNi@CNTs also exhibit excellent OER stability with small current density decay after 12 h.

Results and Discussion:

The synthesis process of the CoFeNi@CNTs electrocatalyst is illustrated in **Scheme 1**. The detailed experimental section could be found in the Supporting Information. We prepared the precursor CoFeNi melamine coordination polymer (CoFeNi MA) using the reflux method, according to literature reported method with small modifications^[39-40]. And the obtained precursor was used as templates to fabricate CoFeNi@CNTs through controllable carbonization and oxidation process. The low-temperature oxidation is aimed at improving the electrical conductivity by forming oxygen vacancies in the materials, thus improving the catalytic performance of the catalysts^[25].



Scheme 1. Illustration of the preparation of CoFeNi@CNTs for the OER

Firstly, scanning electron microscopy (SEM) was utilized to examine the morphologies of the as-synthesized samples. It worth noting that the diameter of the precursor decreases with the iron content increasing (**Figure S1**, Supporting Information). The diameter and length of CoFeNi MA is approximately 80 nm and 1.2 μm , respectively. Interestingly, after two-step calcination, CoFeNi@CNTs possess bamboo-like morphology with wrinkled surface (**Figure 2a and b**). In order to investigate the microscopic morphology and structure of the samples, TEM characterizations were carried out. As we can see from **Figure 2c**, the metal nanoparticles with an average size of

approximately 20 nm are encased in the nanotubes in CoFeNi@CNTs. Moreover, the high-resolution TEM (HRTEM) images (**Figure 2d**) of the CoFeNi@CNTs display that the interplanar spacings of 0.201 nm, 0.202 nm and 0.248 nm which can be indexed into the (101) plane of FeN_{0.056} phase, the (110) plane of Co₃Fe₇ phase and the (311) plane of Fe₃O₄ phase, respectively. We further made EDX elemental mapping for CoFeNi@CNTs, showing a uniform distribution of the C, N elements around the whole nanotube (**Figure 2e**).

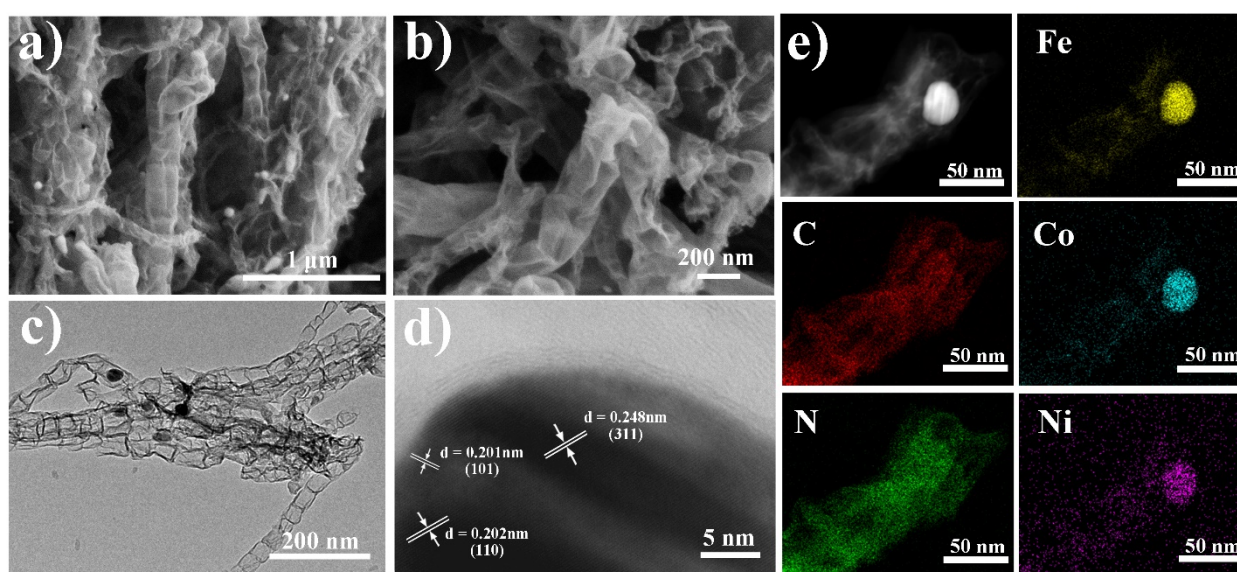


Figure 2. SEM images of CoFeNi@CNTs in a) low magnification and b) high magnification; TEM images of CoFeNi@CNTs in c) low magnification and d) high magnification; e) HADDF-STEM image of CoFeNi@CNTs with EDX mapping.

The X-ray diffraction (XRD) patterns of all the synthesized precursors show sharp and distinct peaks (Figure S3 in the Supporting Information), suggesting the successful fabrication. And the XRD pattern of CoFeNi@CNTs is shown in **Figure 3a**. Its diffraction peaks can be satisfactorily indexed to the Fe₃O₄ phase (JCPDS file no. 88-0866), FeN_{0.056} phase (JCPDS file no.75-2137) and Co₃Fe₇ phase (JCPDS file no. 48-1817). For comparison, the XRD pattern of CoNi@CNTs and FeNi@CNTs were

analyzed. For CoNi@CNTs, the diffraction peaks can be indexed to the CoO phase (JCPDS file no. 72-1474.), CoNiO₂ phase (JCPDS file no. 10-0188) and metallic Ni phase (JCPDS file no. 87-0712). And the pattern for FeNi@CNTs has three main peaks that can be well-indexed to the Fe₃O₄ phase (JCPDS file no. 88-0866), FeN_{0.0324} phase (JCPDS file no. 75-2127) and FeNi alloy phase (JCPDS file no. 37-0474), respectively. The porous structures and pore size distributions of CoFeNi@CNTs were determined by Brunauer–Emmett–Teller (BET) measurements. The sample exhibits a typical type-IV N₂ isotherm and the corresponding specific surface area was 88 m²/g (Figure 3b). Furthermore, the pore size distribution of the sample is mainly centered at ~2.63 nm (insert in Figure 3b), indicating the existence of mesopores.

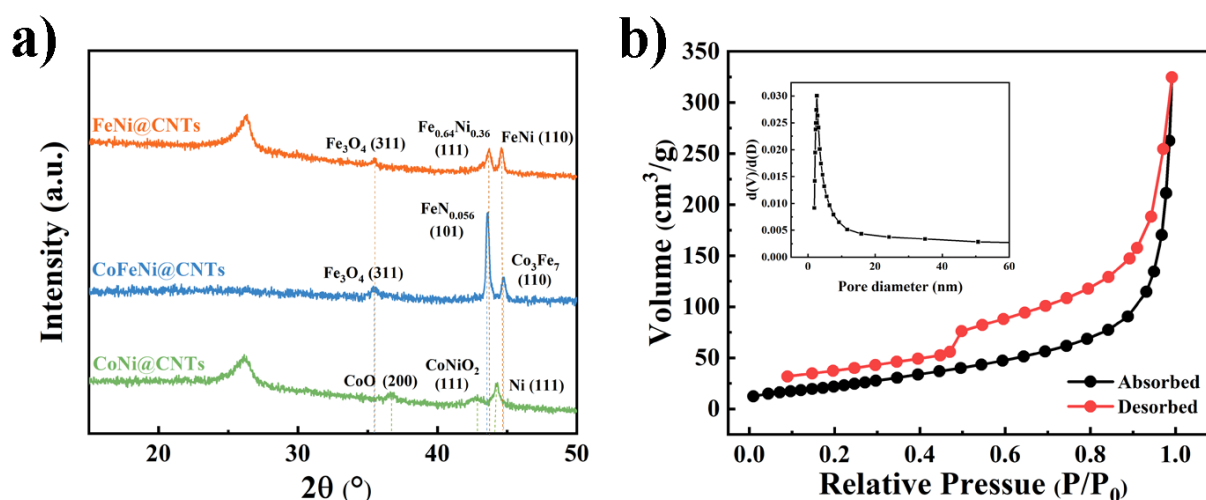


Figure 3. a) XRD patterns of Co/FeNi@CNTs and CoFeNi@CNTs. b) N₂ adsorption–desorption isotherms of CoFeNi@CNTs (inset: pore size distribution).

In order to obtain better confirmation on the graphitization properties of the CoFeNi@CNTs, the Raman spectrum was also conducted. The Raman spectrum of CoFeNi@CNTs displayed two distinct peaks at around 1350 and 1580 cm⁻¹, corresponding to the D band and G band of carbon (Figure S3, Supporting Information). The integrated I_D/I_G ratio of CoFeNi@CNTs is 0.288 approximately,

indicating the high degree of graphitization.

The X-ray photoelectron spectroscopy (XPS) study was carried out to investigate the surface chemical state of the samples and the results are presented in Figure 4a-f, Figure S4 and S5 (seen in the Supporting Information). The survey spectrum in **Figure 4a** reveals that the surface of CoFeNi@CNTs is composed of C, N, Fe, Co and Ni. The C 1s peak spectra can be deconvoluted into three peaks, which correspond to C-C (283.4 eV), C-N (284.2 eV), C-O (288.2 eV) species, as shown in Figure 4b. The existence of C-N bonds indicates that the heteroatom N is successfully doped into the carbon skeleton, while the existence of carbon-oxygen bonds means that the surface of the CoFeNi@CNTs is modified by a large number of oxygen-containing groups, resulting in defects in the matrix^[41]. The N 1s spectra (**Figure 4c**) is deconvoluted into three peaks at 398.1 eV, 400.2 eV and 405.0 eV, which are assigned to pyridinic N, pyrrolic N and graphitic N, respectively. Specifically, the high-resolution XPS spectra of the Fe 2p (**Figure 4d**), Co 2p (**Figure 4e**), and Ni 2p (**Figure 4f**) regions are split into $2p_{3/2}$ and $2p_{1/2}$ doublets due to the spin-orbit coupling. The high-resolution spectrum of Fe $2p_{3/2}$ and Fe $2p_{1/2}$ are positioned at 710.2 eV and 724.0 eV, which can be assigned to the Fe²⁺ in the CoFeNi@CNTs^[42-43]. Similarly, the two spin-orbit doublets of Co 2p are located at 782.3 eV and 796.7 eV, deeming as the Co²⁺ $2p_{3/2}$ and Co²⁺ $2p_{1/2}$ species^[44]. As shown in **Figure 4f**, the core-level signals of Ni located at 852.1 and 873.3 eV are ascribed to Ni $2p_{3/2}$ and Ni $2p_{1/2}$, which can be assigned to Ni²⁺ species^[45-46].

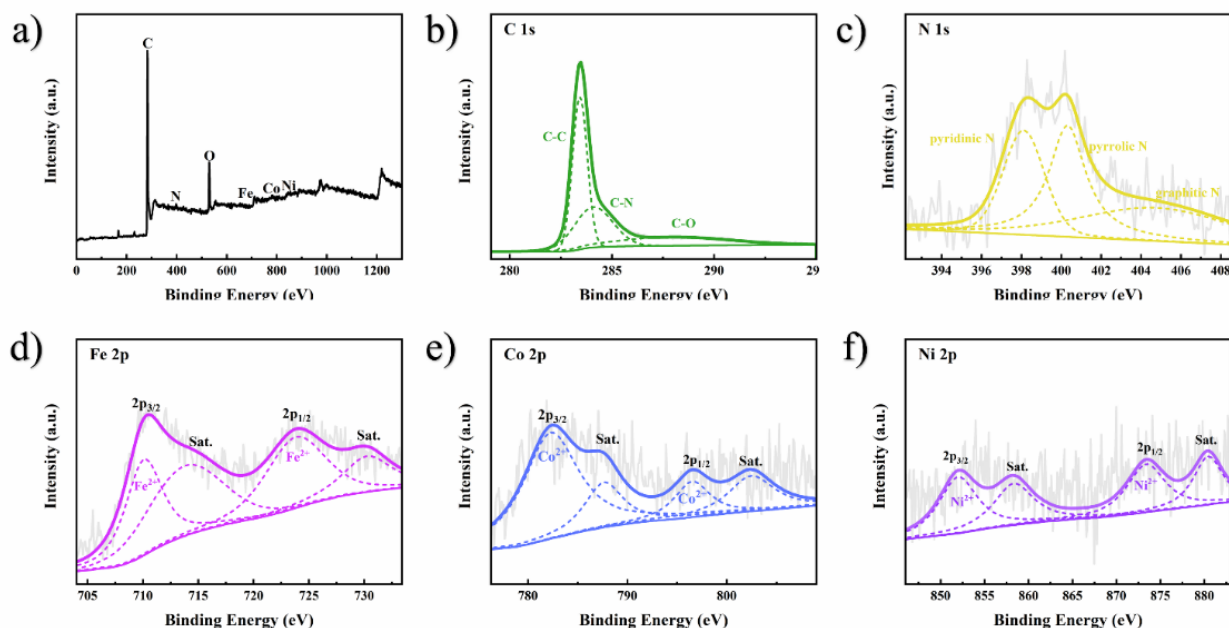


Figure 4. The XPS spectrum of a) survey scan and core-level XPS spectra for the b) C 1s, c) N 1s, d) Fe 2p, e) Co 2p, and f) Ni 2p regions of CoFeNi@CNTs catalyst.

To evaluate the electrocatalytic performance, the OER catalytic activity of CoFeNi@CNTs was carried out in 1 M KOH alkaline electrolyte. For comparison, the samples, including FeNi@CNTs, CoNi@CNTs and the benchmark catalyst IrO₂ were also examined. **Figure 5a** illustrates the linear sweep voltammetry (LSV) curves of all samples with a scan rate of 5 mV s⁻¹ at room temperature. It's worth noting that the CoFeNi@CNTs catalyst possesses the highest OER performance. The overpotential of the CoFeNi@CNTs sample is around 287 mV to reach a current density of 10 mA cm⁻², which is remarkably smaller than that of IrO₂ (355 mV), CoNi@CNTs (392 mV) and FeNi@CNTs (319 mV), revealing the energetical merits of the synergistic effect between three metals. Meanwhile, as shown in **Figure 5b**, CoFeNi@CNTs exhibits the smallest Tafel slopes (32 mV dec⁻¹), while CoNi@CNTs, FeNi@CNTs, and IrO₂ show Tafel slopes of 79, 50, and 38 mV dec⁻¹ respectively, further indicating that for CoFeNi@CNTs, the reaction is kinetically substantially faster with small

mass and electron transport barriers. We also used electrochemical impedance spectroscopy (EIS) to investigate the Nyquist plots of different catalysts (**Figure 5c**). As we expected, the semicircular diameter of CoFeNi@CNTs is markedly smaller than other catalysts, indicating presumably owing to the unique structure and composition of that enables faster mass-transfer. Such an excellent electrocatalytic activity for CoFeNi@CNTs is very outstanding for a nonprecious-metal OER catalyst and even better than those of most reported catalysts (**Table S2**).

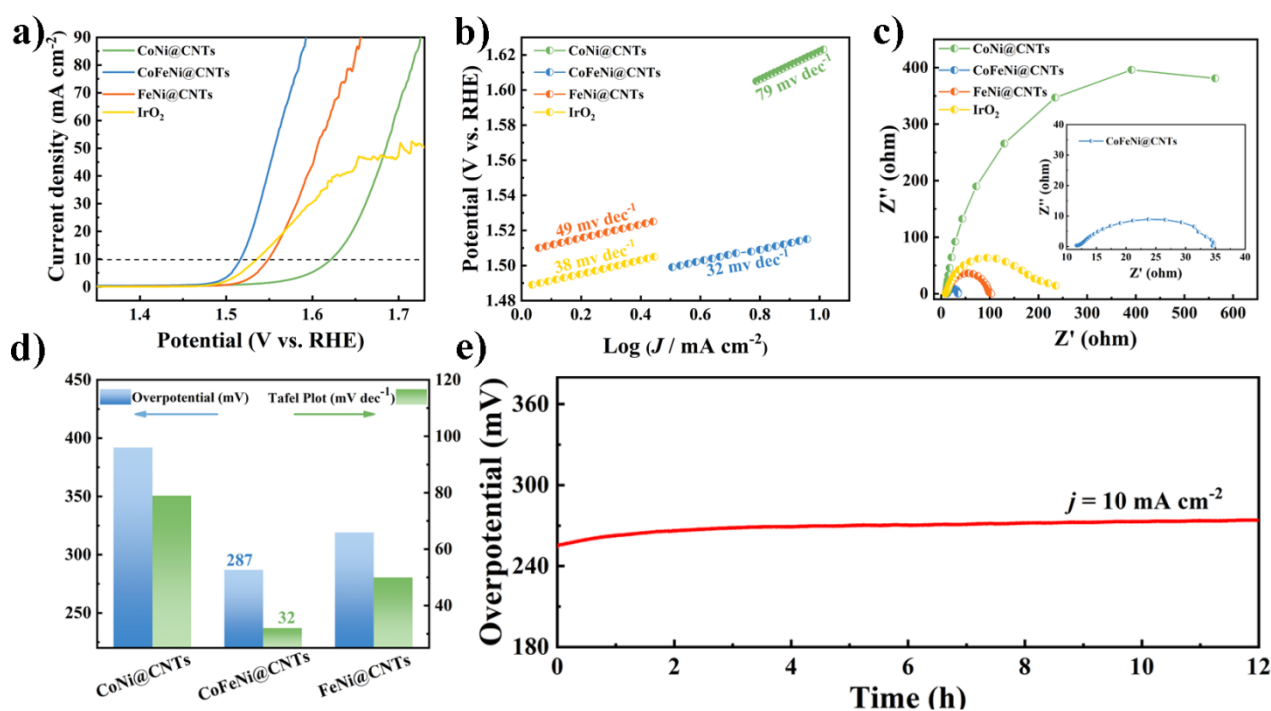


Figure 5. a) LSV curves, b) The corresponding Tafel plots, c) EIS spectra (inset: the EIS spectra of CoFeNi@CNTs), d) summarized overpotentials at $j=10 \text{ mAcm}^{-2}$ and Tafel plots. e) Chronopotentiometric curves of CoFeNi@CNTs with 10 mAcm^{-2} in 1 M KOH;

Besides, the CoFeNi@CNTs is subjected to a CV test for 1000 cycles. The LSV curves of CoFeNi@CNTs show negligible performance loss after the test (Figure S6, Supporting Information). Chronopotentiometric measurement (**Figure 5e**) was further carried out to test the long-term stability of the CoFeNi@CNTs and no apparent electrocatalytic performance attenuation has been observed

after 12 h of reaction. The high durability of CoFeNi@CNTs can be ascribed to its high degree of graphitization and N-doping level.

Conclusion

In summary, we have developed trimetallic N-doped carbon nanotubes as an efficient and stable electrocatalyst for the OER. Doping heteroatoms and an appropriate amount foreign metal atom modified the electronic structure while the unique nanotube structure accelerated electron transport. Moreover, the interaction between alloy nanoparticles and CNTs was highly beneficial for boosting the catalytic activity. And the optimized CoFeNi@CNTs can be used as an efficient OER electrocatalyst with a low overpotential of 287 mV at 10 mA cm⁻² and a Tafel slope of 32 mV dec⁻¹, even outperforming the novel metal-based IrO₂ electrocatalysts. Moreover, the optimized CoFeNi@CNTs exhibits excellent durability for OER with slight activity degradation after continuous electrolysis for 12 h. This work represents an effective strategy, based on coordination polymer precursors, for the design of efficient N-doped carbon nanotubes catalysts for OER. We envision that this strategy will stimulate the exploration of electrocatalysts for wide applications in energy conversion and storage devices.

Acknowledgements

This work was supported by Natural Science Foundation of Zhejiang Province (No. LY19E020007). J. G. acknowledges the financial support from the Fundamental Research Funds of Zhejiang Sci-Tech University (2019Q007).

References

- [1] H. Xia, Q. Xu, J. Zhang, *Nano-Micro Lett.* **2018**, *10*, 66.
- [2] Y. Ma, X. Dong, Y. Wang, Y. Xia, *Angew. Chem. Int. Ed.* **2018**, *57*, 2904-2908.
- [3] J. Y. Zhang, H. Wang, Y. Tian, Y. Yan, Q. Xue, T. He, H. Liu, C. Wang, Y. Chen, B. Y. Xia, *Angew. Chem. Int. Ed.* **2018**, *57*, 7649-7653.
- [4] H. Khani, N. S. Grundish, D. O. Wipf, J. B. Goodenough, *Adv. Energy Mater.* **2019**, *10*, 1903215.
- [5] Y. Wang, J. Li, Z. Wei, *J. Mater. Chem. A* **2018**, *6*, 8194-8209.
- [6] J. Wang, Z. Wei, H. Wang, Y. Chen, Y. Wang, *J. Mater. Chem. A* **2017**, *5*, 10510-10516.
- [7] N.-T. Suen, S.-F. Hung, Q. Quan, N. Zhang, Y.-J. Xu, H. M. Chen, *Chem. Soc. Rev.* **2017**, *46*, 337-365.
- [8] D. Ji, L. Fan, L. Tao, Y. Sun, M. Li, G. Yang, T. Q. Tran, S. Ramakrishna, S. Guo, *Angew. Chem. Int. Ed.* **2019**, *58*, 13840-13844.
- [9] X.-T. Wang, T. Ouyang, L. Wang, J.-H. Zhong, T. Ma, Z.-Q. Liu, *Angew. Chem. Int. Ed.* **2019**, *58*, 13291-13296.
- [10] X. Xiao, C.-T. He, S. Zhao, J. Li, W. Lin, Z. Yuan, Q. Zhang, S. Wang, L. Dai, D. Yu, *Energy Environ. Sci.* **2017**, *10*, 893-899.
- [11] Y. Li, H. Zhang, M. Jiang, Y. Kuang, X. Sun, X. Duan, *Nano Res.* **2016**, *9*, 2251-2259.
- [12] X. Li, X. Wang, J. Zhou, L. Han, C. Sun, Q. Wang, Z. Su, *J. Mater. Chem. A* **2018**, *6*, 5789-5796.
- [13] K. Zhu, X. Zhu, W. Yang, *Angew. Chem. Int. Ed.* **2019**, *58*, 1252-1265.
- [14] T. Tarnev, H. B. Aiyappa, A. Botz, T. Erichsen, A. Ernst, C. Andronescu, W. Schuhmann, *Angew. Chem. Int. Ed.* **2019**, *58*, 14265-14269.
- [15] J. Huang, Y. Li, Y. Zhang, G. Rao, C. Wu, Y. Hu, X. Wang, R. Lu, Y. Li, J. Xiong, *Angew. Chem. Int. Ed.* **2019**, *58*, 17458-17464.
- [16] S.-H. Yu, Y. Duan, Y. Zi-You, S.-j. Hu, X.-S. Zheng, C.-T. Zhang, H. Ding, B.-C. Hu, Q. Fu, Z.-L. Yu, X. Zheng, J. Zhu, M.-R. Gao, *Angew. Chem. Int. Ed.* **2019**, *58*, 15772-15777.
- [17] J. Yang, X. Zhou, D. Wu, X. Zhao, Z. Zhou, *Adv. Mater.* **2017**, *29*, 1604108.
- [18] W. Alkarmo, F. Ouhib, A. Aqil, J.-M. Thomassin, B. Vertruyen, M.-L. Piedboeuf, N. Job, C.

- Detrembleur, C. Jérôme, *J. Mater. Sci.* **2018**, *53*, 6135-6146.
- [19] K. Gao, B. Wang, L. Tao, B. V. Cunnig, Z. Zhang, S. Wang, R. S. Ruoff, L. Qu, *Adv. Mater.* **2019**, *31*, 1805121.
- [20] P. Yan, J. Liu, S. Yuan, Y. Liu, W. Cen, Y. Chen, *Appl. Surf. Sci.* **2018**, *445*, 398-403.
- [21] Q. Li, H. Pan, D. Higgins, R. Cao, G. Zhang, H. Lv, K. Wu, J. Cho, G. Wu, *Small* **2015**, *11*, 1443-1452.
- [22] Y. Guo, P. Yuan, J. Zhang, H. Xia, F. Cheng, M. Zhou, J. Li, Y. Qiao, S. Mu, Q. Xu, *Adv. Funct. Mater.* **2018**, *28*, 1805641.
- [23] J.-X. Feng, H. Xu, Y.-T. Dong, X.-F. Lu, Y.-X. Tong, G.-R. Li, *Angew. Chem. Int. Ed.* **2017**, *56*, 2960-2964.
- [24] a) C. Li, H. Xu, J. Gao, W. Du, L. Shangguan, X. Zhang, R.-B. Lin, H. Wu, W. Zhou, X. Liu, J. Yao, B. Chen, *J. Mater. Chem. A* **2019**, *7*, 11928-11933; b) J. Wen, Y. Li, J. Gao, *Chem. Res. Chin. Univ.* **2020**, DOI: 10.1007/s40242-40020-40163-40246; c) Y. Yan, C. Li, Y. Wu, J. Gao, Q. Zhang, *J. Mater. Chem. A* **2020**, DOI: 10.1039/D1030TA03749D; d) J. Gao, X. Qian, R. Lin, R. Krishna, H. Wu, W. Zhou, B. Chen, *Angew. Chem. Int. Ed.* **2020**, *59*, 4396-4400.
- [25] M. Lu, X. Yang, Y. Li, Z. Zhu, Y. Wu, H. Xu, J. Gao, J. Yao, *Chem. Asian J.* **2019**, *14*, 3357-3362.
- [26] Y. Wu, H. Chen, J. Wang, H. Liu, E. Lv, Z. Zhu, J. Gao, J. Yao, *ChemNanoMat* **2019**, *6*, 107-112.
- [27] T. Zhao, J. Gao, J. Wu, P. He, Y. Li, J. Yao, *Energy Technol.* **2019**, *7*, 1800969.
- [28] L. Wang, H. Xu, J. Gao, J. Yao, Q. Zhang, *Coord. Chem. Rev.* **2019**, *398*, 213016.
- [29] Y. Feng, X.-Y. Yu, U. Paik, *Sci. Rep.* **2016**, *6*, 34004.
- [30] H. Ning, G. Li, Y. Chen, K. Zhang, Z. Gong, R. Nie, W. Hu, Q. Xia, *ACS Appl. Mater. Interfaces* **2019**, *11*, 1957-1968.
- [31] P. Zhao, X. Hua, W. Xu, W. Luo, S. Chen, G. Cheng, *Catal. Sci. Technol.* **2016**, *6*, 6365-6371.
- [32] B. Y. Xia, Y. Yan, N. Li, H. B. Wu, X. W. D. Lou, X. Wang, *Nat. Energy* **2016**, *1*, 15006.
- [33] J. S. Li, S. L. Li, Y. J. Tang, M. Han, Z. H. Dai, J. C. Bao, Y. Q. Lan, *Chem. Commun.* **2015**, *51*, 2710-2713.
- [34] W.-L. Xin, K.-K. Lu, D.-R. Zhu, H.-B. Zeng, X.-J. Zhang, R.-S. Marks, D. Shan, *Electrochim. Acta* **2019**, *307*, 375-384.

- [35] X. Zhao, B. Pattengale, D. Fan, Z. Zou, Y. Zhao, J. Du, J. Huang, C. Xu, *ACS Energy Lett.* **2018**, *3*, 2520-2526.
- [36] Z. Tao, T. Wang, X. Wang, J. Zheng, X. Li, *ACS Appl. Mater. Interfaces* **2016**, *8*, 35390-35397.
- [37] J. Diao, Y. Qiu, S. Liu, W. Wang, K. Chen, H. Li, W. Yuan, Y. Qu, X. Guo, *Adv. Mater.* **2020**, *32*, 1905679.
- [38] J. Sun, S. E. Lowe, L. Zhang, Y. Wang, K. Pang, Y. Wang, Y. Zhong, P. Liu, K. Zhao, Z. Tang, H. Zhao, *Angew. Chem. Int. Ed.* **2018**, *57*, 16511-16515.
- [39] a) J. Cong, C. Li, T. Zhao, J. Wu, R. Zhang, W. Ren, S. Wang, J. Gao, Y. Liu, J. Yao, *J. Solid State Chem.* **2017**, *253*, 227-230; b) Y. Li, M. Lu, Y. Wu, H. Xu, J. Gao, J. Yao, *Adv. Mater. Interfaces* **2019**, *6*, 1900290; c) Y. Li, T. Zhao, M. Lu, Y. Wu, Y. Xie, H. Xu, J. Gao, J. Yao, G. Qian, Q. Zhang, *Small* **2019**, *15*, 1901940.
- [40] C. Chen, C.-W. Yeh, J.-D. Chen, *Polyhedron* **2006**, *25*, 1307-1312.
- [41] a) C. Y. Su, H. Cheng, W. Li, Z. Q. Liu, N. Li, Z. Hou, F. Q. Bai, H. X. Zhang, T. Y. Ma, *Adv. Energy Mater.* **2017**, *7*, 1602420; b) S. B. Maddinedi, J. Sonamuthu, S. S. Yildiz, G. Han, Y. Cai, J. Gao, Q. Ni, J. Yao, *J. Photochem. Photobiol. B* **2018**, *186*, 189-196.
- [42] Y. Teng, X. D. Wang, J. F. Liao, W. G. Li, H. Y. Chen, Y. J. Dong, D. B. Kuang, *Adv. Funct. Mater.* **2018**, *28*, 1802463.
- [43] S. Zhao, M. Li, M. Han, D. Xu, J. Yang, Y. Lin, N. E. Shi, Y. Lu, R. Yang, B. Liu, *Adv. Funct. Mater.* **2018**, *28*, 1706018.
- [44] Y. Pi, Q. Shao, P. Wang, F. Lv, S. Guo, J. Guo, X. Huang, *Angew. Chem. Int. Ed.* **2017**, *56*, 4502-4506.
- [45] Q. Wang, L. Shang, R. Shi, X. Zhang, Y. Zhao, G. I. Waterhouse, L. Z. Wu, C. H. Tung, T. Zhang, *Adv. Energy Mater.* **2017**, *7*, 1700467.
- [46] L. Zhou, M. Shao, C. Zhang, J. Zhao, S. He, D. Rao, M. Wei, D. G. Evans, X. Duan, *Adv. Mater.* **2017**, *29*, 1604080.

Table of Contents Only

Trimetallic N-doped carbon nanotubes with rapid electron transport and rapid diffusion of the electrolyte was synthesized through a pyrolysis-oxidation process. The synergistic cooperation between trimetallic components as well as the unique carbon nanotube structure endow the CoFeNi@CNTs electrocatalysts with excellent OER activity and outstanding durability.

